

## Supporting information

### **Additive and Base free Tandem Aerobic Oxidative Cleavage of Olefins to Esters using Bifunctional Mesoporous Copper Incorporated Al-SBA-15**

Krishnan Ravi<sup>ab</sup>, Yash S. Dalal<sup>a</sup>, Anjana C. Sabu <sup>a</sup>, Mohd Shadab A. Khalifa <sup>a</sup>, Ankush V. Biradar<sup>ab\*</sup>

<sup>a</sup>Inorganic Materials and Catalysis Division, CSIR-Central Salt & Marine Chemicals Research Institute, G. B. Marg, Bhavnagar-364 002, Gujarat, India

<sup>b</sup>Academy of Scientific and Innovative Research (AcSIR), Ghaziabad-201 002, India

E-mail: [ankush@csmcri.res.in](mailto:ankush@csmcri.res.in)

*Corresponding author: Tel.: Dr. Ankush +91 278 2567760 Ext: 7170; Fax: +91 278 2566970*

# **Contents**

<b>Contents</b>	<b>Page. No.</b>
<b>Experimental section</b>	
1. Physicochemical methods	S3,S4
2. Catalysis synthesis and catalytic activity	S5
<b>Table S1</b> Aerobic oxidation of styrene to benzaldehyde using mesoporous silica materials	S6
<b>Table S2</b> One-pot two step oxidative esterification of olefins to esters using homogeneous/heterogeneous catalyst	S7
<b>Figure S1.</b> Low angle PXRD spectra of Al-SBA-15	S8
<b>Figure S2.</b> CO <sub>2</sub> -TPD spectrum of 10Cu-Al-SBA-15	S9
<b>Figure S3.</b> High-resolution XPS spectra O 1s of the 10Cu-Al-SBA-15	S10
<b>Figure S4.</b> (a) Survey spectra of the spent 10Cu-Al-SBA-15 catalyst. High-resolution XPS spectra (b) Cu 2p peak, (c) Al 2p peak, (d) Si 2p of the 10Cu-Al-SBA-15	S11
<b>Figure S5.</b> GC-MS spectrum of isophthalaldehyde	S12
<b>Figure S6.</b> GC-MS spectrum of 4-chlorobenzaldehyde	S12
<b>Figure S7.</b> GC-MS spectrum of 4-methylbenzaldehyde	S12
<b>Figure S8.</b> GC-MS spectrum of isopropyl benzoate	S12
<b>Figure S9.</b> GC-MS spectrum of methyl benzoate	S12
<b>Figure S10.</b> GC-MS spectrum of propyl benzoate	S13
<b>Figure S11.</b> GC-MS spectrum of butyl benzoate	S13

## S1. Experimental section

### S1.1 Physicochemical Methods

Powder X-ray diffraction (PXRD) data were obtained using a PANalytical Empyrean (PIXcel 3D detector) system equipped with Cu K $\alpha$  ( $\lambda=1.54 \text{ \AA}$ ) radiation. The operating voltage and current were 40 kV and 30 mA, respectively. A step size of  $0.04^\circ$  with a step time of 2 seconds was used for data collection. FTIR analysis of the samples was recorded on self-supporting wafers prepared as KBr pellets using a Perkin-Elmer GX FTIR spectrometer in the region of  $400\text{--}4000 \text{ cm}^{-1}$  with KBr in a 1:20 weight ratio. The morphology of the synthesized catalyst was obtained by Scanning Electron Microscopy (SEM) images which were recorded on a JEOL JSM 7100F microscope, using an accelerating voltage of 18 kV and a probe current of 102 A. Samples were prepared by dispersing in isopropyl alcohol (IPA), and a drop of the suspension added to the SEM copper grid. The transmission electron microscopy (TEM), high-resolution TEM observation was acquired on JEOL, JEM 2100 with an electron acceleration energy of 200 kV. The samples were ultrasonically dispersed in IPA for 30 min and deposited on the carbon coated Lacey 200 mesh Cu grid and dried overnight. Specific surface area and pore size analysis of the samples were measured by nitrogen adsorption at  $-196 \text{ }^\circ\text{C}$  using a sorptometer (ASAP-2010, Micromeritics). The samples were degassed under vacuum at  $200 \text{ }^\circ\text{C}$  for 3h before measurements to expel the interlayer water molecules. The X-ray photoelectron spectroscopy (XPS) measurements were performed on a Thermo Fisher Nexsa spectrometer equipped with monochromatic Al K $\alpha$  radiation of energy 1486.6 eV. The pass energy for the survey was set at 400 eV and the pass energy for the narrow scan was set at 50 eV. The dual-beam charge neutralization was used for both low-energy electrons and ions. The sample surface is at a  $90^\circ$  angle with the axis of the input lens. Further, the individual core-level spectra were checked for charging using C1s at 284.8 eV as standard and corrected if needed. The peak fitting of the individual core levels was done using Avantage software. Hydrogen Temperature Programmed Reduction ( $\text{H}_2$ -TPR) analysis data were obtained using Micromeritics® Autochem II 2920 instrument. In the U-shaped quartz tube, 0.1 g of sample was placed over a layer of quartz wool. The catalyst was purged first with helium flow for 2 h and then cooled to ambient temperature. The catalysts were then exposed to a  $50 \text{ mL}\cdot\text{min}^{-1}$  flow of 20%  $\text{H}_2$  in helium as the temperature was linearly increased to  $900 \text{ }^\circ\text{C}$  at a  $10 \text{ }^\circ\text{C}\cdot\text{min}^{-1}$  ramping rate. The thermal conductivity detector (TCD) observed the changes in the effluent's  $\text{H}_2$  concentration.

Temperature-Programmed Desorption (TPD) of CO<sub>2</sub> was also performed on the Micrometrics® Autochem II 2920 instrument. 0.1 g of sample was placed in the U-shaped quartz tube over a layer of quartz wool. First, 25 mL.min<sup>-1</sup> of helium flow was introduced for 60 min at 200 °C with a 5 °C.min<sup>-1</sup> ramp rate. Afterward, the sample was cooled in 50 mL.min<sup>-1</sup> helium flow till 100 °C. For adsorption of NH<sub>3</sub> and CO<sub>2</sub>, 40 mL.min<sup>-1</sup> flow of CO<sub>2</sub> in helium was introduced into the reactor at 100 °C for 30 min. Then, 40 mL.min<sup>-1</sup> of helium flow was fed for 60 min to get rid of physically adsorbed species. Finally, desorption was studied with 5 °C.min<sup>-1</sup> heating rate until 850 °C. Gases were analyzed on a TCD, with helium used as a reference gas. The reaction mixture was collected and analyzed using a gas chromatography system equipped with FID as a detector (GC-7890B-Agilent) with HP-5 column, consisting of 5% diphenyl and 95% dimethyl polysiloxane capillary stationary phase and nitrogen as the carrier gas. The appropriate diluted reaction mixture with tetradecane as an internal standard and analyzed on GC and a gas chromatography-mass spectrometry (equipped with FID as a detector (GC-MS Shimadzu, QP-2010, Japan) with HP-5 column which consists of 5% diphenyl and 95% dimethyl polysiloxane capillary phase with helium as the carrier gas. The ramp rate of initially 50 °C hold for 3 mins, 20 °C ramp to 320 °C with 20 mins hold).

## **S2. Catalysis synthesis and catalytic activity**

### **S2.1 Synthesis of Co-Al-SBA-15**

The Co-Al-SBA-15 was synthesized by simple impregnation methods. In a 50 mL polypropylene bottle, 0.2 g of Al-SBA-15 and 0.098 g  $\text{Co}(\text{NO}_3)_2 \cdot 6\text{H}_2\text{O}$  dissolved into 10 mL deionized water and constantly stirred for 24 h at 400 rpm. After 24 h, the water is evaporated through rota evaporation and dried at 80 °C overnight. Finally, the catalyst was calcined at 550 °C at 5 h (2 °C/min) and denoted 2Cu-Al-SBA-15, 5 Cu-Al-SBA-15, and 10 Cu-Al-SBA-15, respectively.

### **S2.2 Oxidation of styrene to benzaldehyde**

In a 15 mL glass tube, 2.40 mmol of styrene, 0.025 g of Cu-Al-SBA-15, 1 mL GVL added and heated at different temperatures while stirring at 400 rpm for about 12 to 24 h. After the reaction, the reaction mixture is centrifuged to separate the catalyst. Further, the liquid product was analyzed by GC and GC-MS.

### **S2.3 Esterification of benzoic acid with different alcohols**

In a 30 mL glass tube, 2.40 mmol of styrene, 0.025 g of Cu-Al-SBA-15, 1 mL solvent added and heated at different temperatures while stirring at 400 rpm for about 12 to 24 h. After the reaction, the reaction mixture is centrifuged to separate the catalyst. Further, the liquid product was analyzed by GC and GC-MS.

#### **Conversion and selectivity calculated by GC**

**Conversion (%)** =  $[(\text{Initial mol}\%) - (\text{Final mol}\%)] / (\text{Initial mol}\%)$

**Selectivity (%)** =  $[(\text{moles of product formed}) / (\text{moles of substrate consumed})] * 100$

### S3. Aerobic oxidation of styrene to benzaldehyde using mesoporous silica materials

Table S1 Aerobic oxidation of styrene to benzaldehyde using mesoporous silica materials						
Sr. No.	Catalyst	Oxidant Additives	Reaction conditions	Conv. (%)	Sel./yield of benzaldehyde (%)	Ref.
1	Cu-Mn/SBA-15	TBHP	Styrene (10 mmol), TBHP (40 mmol), Cu-Mn/SBA-15 (20 mg), acetonitrile (10 mL), 7 h at 80 °C.	97.3	20	1
2	HCS-50	H <sub>2</sub> O <sub>2</sub>	Styrene (1 mmol), H <sub>2</sub> O <sub>2</sub> (1.0 g), HCS-50 (50 mg), 24 h at RT.	100	42.24%	2
3	Fe <sub>3</sub> O <sub>4</sub> @SiO <sub>2</sub> @mSiO <sub>2</sub> -Fe	H <sub>2</sub> O <sub>2</sub>	Styrene (10 mmol), H <sub>2</sub> O <sub>2</sub> (10 mmol), Fe <sub>3</sub> O <sub>4</sub> @SiO <sub>2</sub> @mSiO <sub>2</sub> -Fe (100 mg), acetonitrile (10 mL), 10 h at 60 °C.	52.8	84.9%	3
4	IMM-TMCl-Ni(II)	H <sub>2</sub> O <sub>2</sub>	Styrene (1 mol), H <sub>2</sub> O <sub>2</sub> (4 mol), F IMM-TMCl-Ni(II) (500 mg), acetonitrile (8 g), 6 h at 70 °C.	36.8	93.6	4
5	V-SBA-16	TBHP	Styrene (2.6 mmol), TBHP (2.6 mmol), V-SBA-16 (50 mg), acetonitrile (10 mL), 24 h at 80 °C.	83.9	55.5	5
6	PMo11Co/SBA	O <sub>2</sub> /IBA	Styrene (1 mmol), Air (10 ml/min), PMo11Co/SBA (10 mg), IBA (2 mmol), 1 h at 40 °C.	89	15	6
7	Ti-Fe-SBA-15	H <sub>2</sub> O <sub>2</sub>	Styrene (15 mmol), H <sub>2</sub> O <sub>2</sub> (75 mmol), Ti-Fe-SBA-15 (100 mg), acetonitrile (16 mL), 12 h at 70 °C.	37	86	7
8	10Cu-Al-SBA-15	O <sub>2</sub>	Styrene (2.40 mmol), 10Cu-Al-SBA-15 (25 mg), 1 mL GVL and 1 atm O <sub>2</sub> at 120 °C for 24 h	100	6	This work

HCS-50: Trivalent ceria-silica composite, IMM-TMCl-Ni(II): Ni<sup>2+</sup>-containing ionic liquid (IL) 1-methyl-3-[(triethoxysilyl)propyl] imidazolium chloride (TMCl) immobilized on silica, IBA: isobutyraldehyde

#### References

- V. Chaudhary, Synthesis and catalytic activity of SBA-15 supported catalysts for styrene oxidation. *Chin. J. Chem. Eng.*, 2018, **26**, 1300-1306.
- N. Pal, E. B. Cho, D. Kim, C. Gunathilake, M. Jaroniec, Catalytic activity of CeIVO<sub>2</sub>/Ce<sub>2</sub>III<sub>2</sub>O<sub>3</sub>-silica mesoporous composite materials for oxidation and esterification reactions. *Chem. Eng. J.*, 2015, **262**, 1116-1125.
- Y. Yang, B. Xu, J. He, J. Shi, L. Yu, Y. Fan, Design and synthesis of Fe<sub>3</sub>O<sub>4</sub>@ SiO<sub>2</sub>@ mSiO<sub>2</sub>-Fe: A magnetically separable catalyst for selective oxidative cracking reaction of styrene using air as partial oxidant. *Appl. Catal. A: Gen.*, 2020, **590**, 117353.
- G. Liu, M. Hou, J. Song, Z. Zhang, T. Wu, B. Han, Ni<sup>2+</sup>-containing ionic liquid immobilized on silica: Effective catalyst for styrene oxidation with H<sub>2</sub>O<sub>2</sub> at solvent-free condition. *J. Mol. Catal. A: Chem.*, 2010, **316**, 90-94.
- B. R. Jermy, S. Y. Kim, K. V. Bineesh, D. W. Park, Optimization, synthesis and characterization of vanadium-substituted thick-walled three-dimensional SBA-16. *Microporous Mesoporous Mater.*, 2009, **117**, 661-669.
- X. Song, W. Zhu, K. Li, J. Wang, H. Niu, H. Gao, W. Gao, W. Zhang, J. Yu, M. Jia, Epoxidation of olefins with oxygen/isobutyraldehyde over transition-metal-substituted phosphomolybdic acid on SBA-15. *Catal. Today*, 2016, **259**, 59-65.
- Y. Wu, Y. Zhang, J. Cheng, Z. Li, H. Wang, Q. Sun, B. Han, Y. Kong, Synthesis, characterization and catalytic activity of binary metallic titanium and iron containing mesoporous silica. *Microporous Mesoporous Mater.*, 2012, **162**, 51-59.

### S3.1 One-pot two step oxidative esterification of olefins to esters using homogeneous/heterogeneous catalyst

Table S2 One-pot two step oxidative esterification of olefins to esters using homogeneous/heterogeneous catalyst						
Sr. No.	Catalyst	Oxidant Additives	Reaction conditions	Conv. (%)	Sel./yield(%)	Ref.
1 <sup>a</sup>	1,2-dibutoxyethane	O <sub>2</sub> , N,N'-dicyclohexylcarbodiimide	Styrene (0.6 mmol), solvent (4 equiv), heat, O <sub>2</sub> balloon, 12 h. (Step-1) and MeOH (0.6 mmol), N,N'-dicyclohexylcarbodiimide (0.9 mmol) and 4-dimethylaminopyridine (0.3 mmol), 8 h at RT. (Step-2)	-	85	1
2 <sup>b</sup>	Tubular carbon nitride	O <sub>2</sub> and HCl	Styrene: (0.5 mmol), TCN (10 mg), and HCl (0.3 mL, 37 wt% aqueous) in MeOH (2 mL) were irradiated with a 250 W Xe lamp under oxygen at RT for 10 h	-	77	2
3 <sup>c</sup>	Fe-NC-900	TBHP	Styrene (0.25 mmol), Fe-NC-900 (10 mol%), K <sub>2</sub> CO <sub>3</sub> (20 mol%), TBHP (2.2 equiv.), MeOH (4 mL), 1.0 MPa O <sub>2</sub> , 48 h, 150 °C.	-	84	3
4 <sup>c</sup>	10Cu-Al-SBA-15	O <sub>2</sub>	<b>Styrene (2.40 mmol), 10Cu-Al-SBA-15 (0.25 g), 1 mL GVL and 1 atm O<sub>2</sub> at 120 °C for 24 h, 600 rpm (Step-1). Further, 1 mL of MeOH added without addition of O<sub>2</sub> for 24 h at 65 °C, 600 rpm.</b>	<b>100</b>	<b>66</b>	<b>This work</b>
<sup>a</sup> Homogeneous catalyst system, <sup>b</sup> photocatalytic conversion, <sup>c</sup> thermochemical catalytic conversion						

#### References

1. J. Ou, H. Tan, S. He, W. Wang, B. Hu, G. Yu, K. Liu, 1, 2-Dibutoxyethane-Promoted Oxidative Cleavage of Olefins into Carboxylic Acids Using O<sub>2</sub> Under Clean Conditions. *J. Org. Chem.*, 2021, **86**, 14974-14982.
2. H. Wang, R. Jia, M. Hong, H. Miao, B. Ni, T. Niu, Hydroxyl radical-mediated oxidative cleavage of C=C bonds and further esterification reaction by heterogeneous semiconductor photocatalysis. *Green Chem.*, 2021, **23**, 6591-6597.
3. X. Yu, Z. Zhao, L. Zhu, S. Tan, W. Fu, L. Wang, Y. An, Aerobic oxidative cleavage and esterification of C=C bonds catalyzed by iron-based nanocatalyst. *Mol. Catal.*, 2022, **519**, 112152.

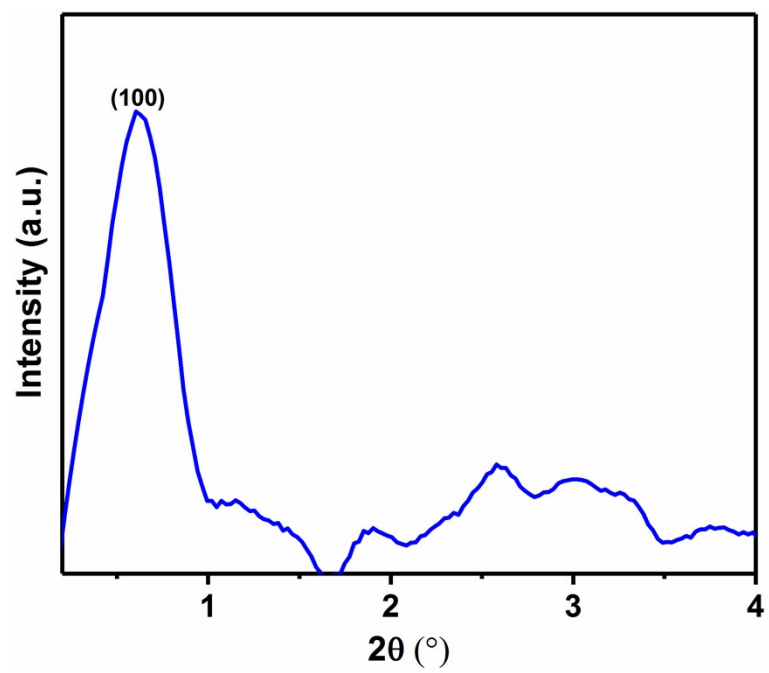


**Fig. S1** Low angle PXRD spectra of Al-SBA-15

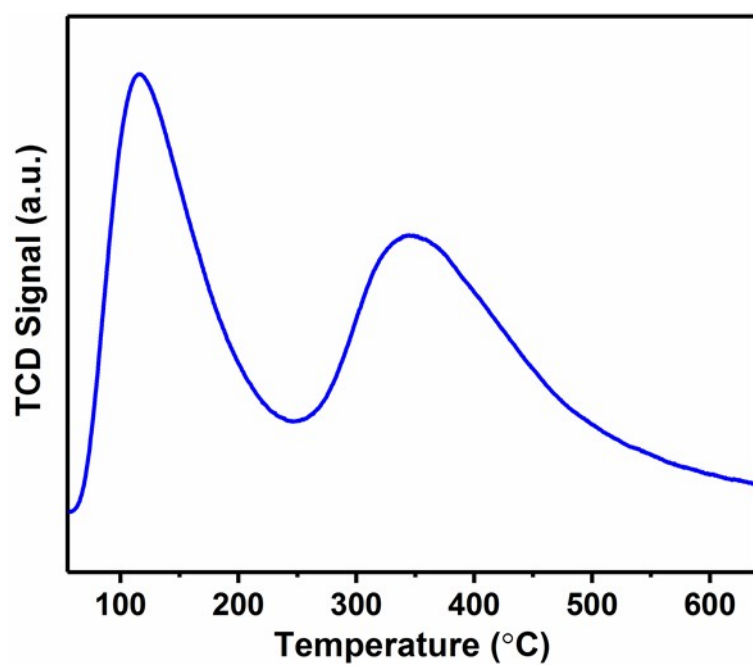


**Fig. S2** CO<sub>2</sub>-TPD spectrum of 10Cu-Al-SBA-15

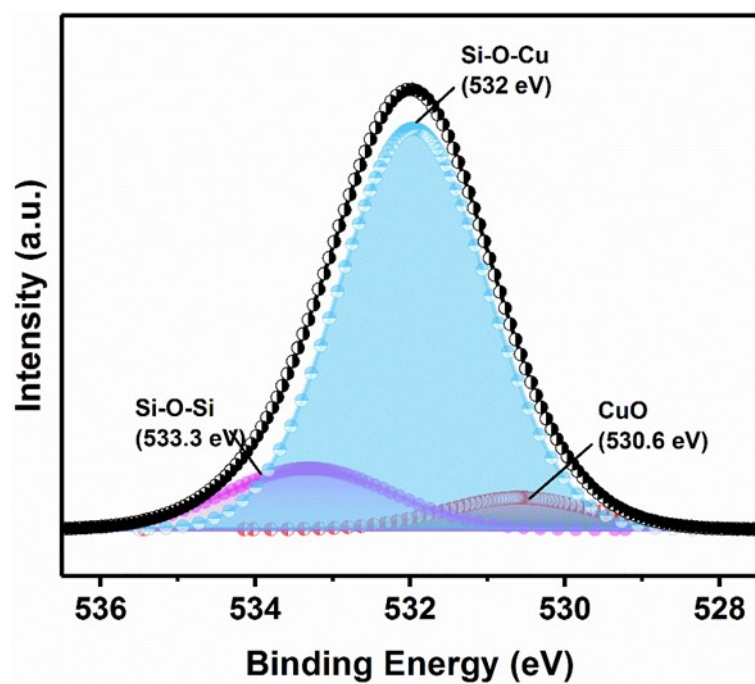


**Fig. S3** High-resolution XPS spectra O 1s of the 10Cu-Al-SBA-15

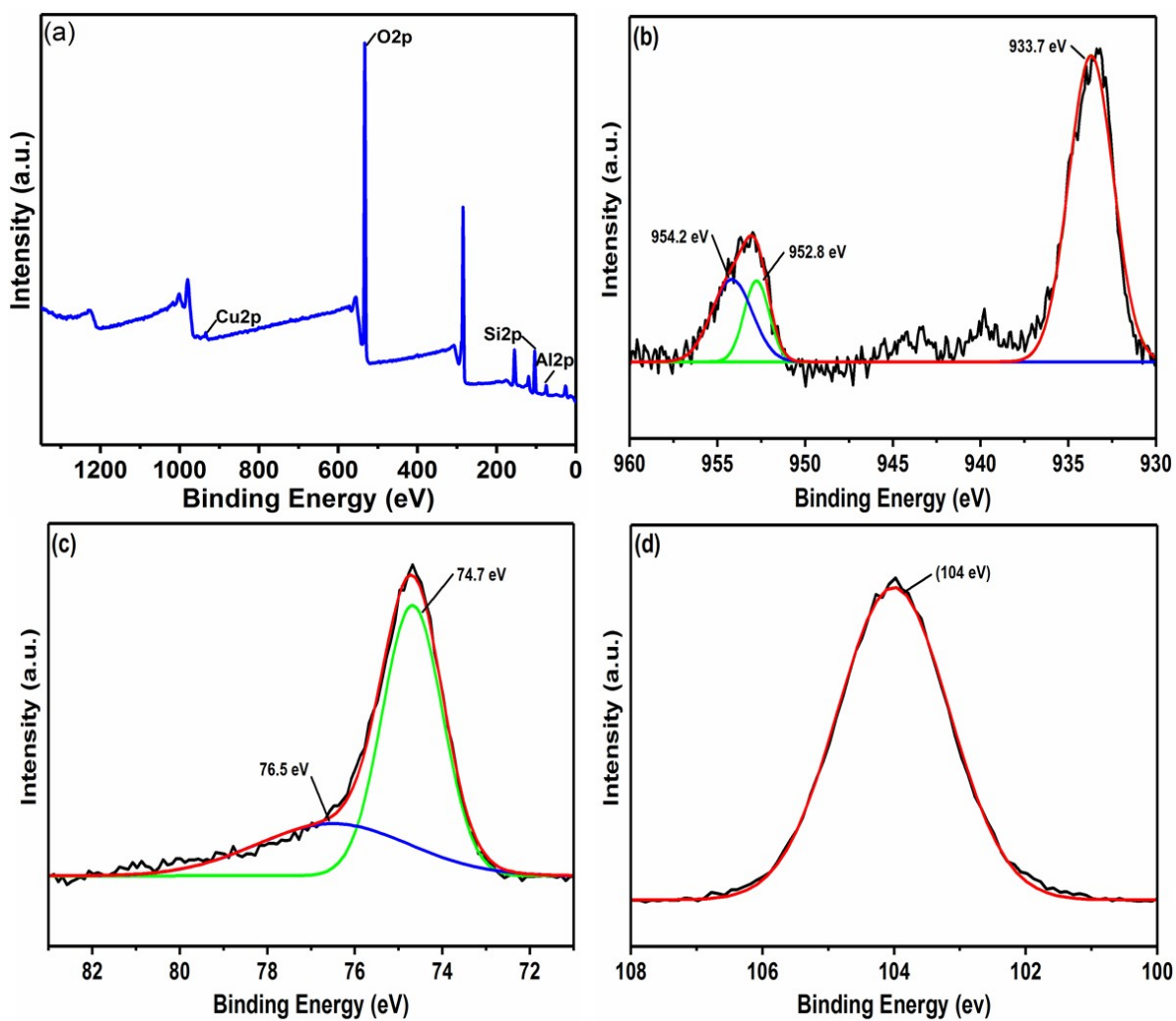


**Fig. S4** (a) Survey spectra of the spent 10Cu-Al-SBA-15 catalyst. High-resolution XPS spectra (b) Cu 2p peak, (c) Al 2p peak, (d) Si 2p of the 10Cu-Al-SBA-15.

#### S4. GC-MS spectrum

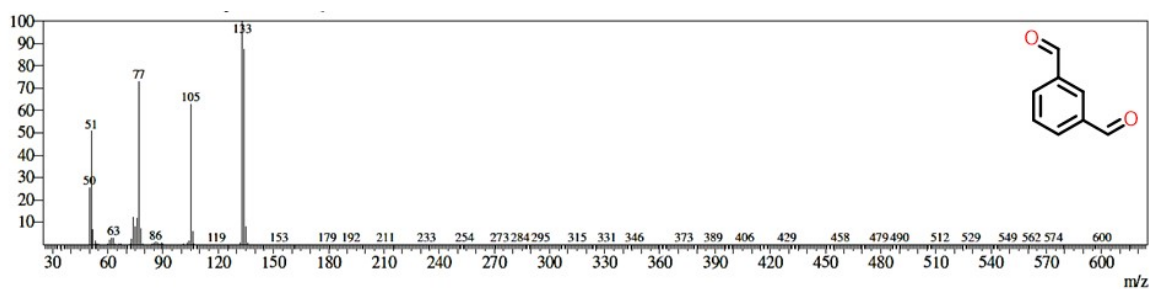


Fig. S5 GC-MS spectrum of isophthalaldehyde

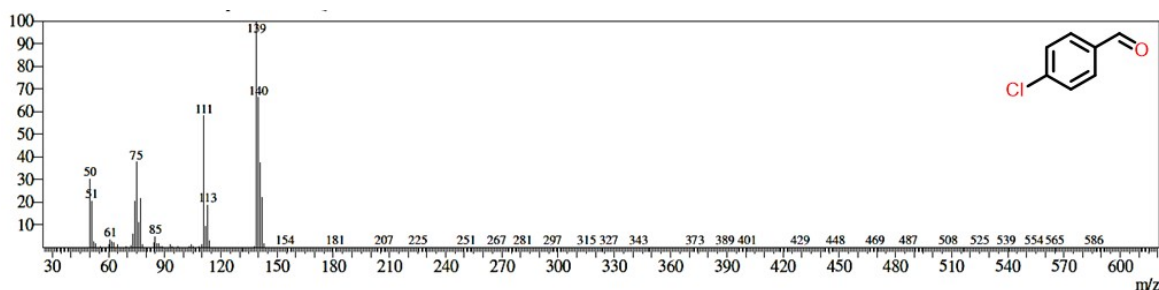


Fig. S6 GC-MS spectrum of 4-chlorobenzaldehyde

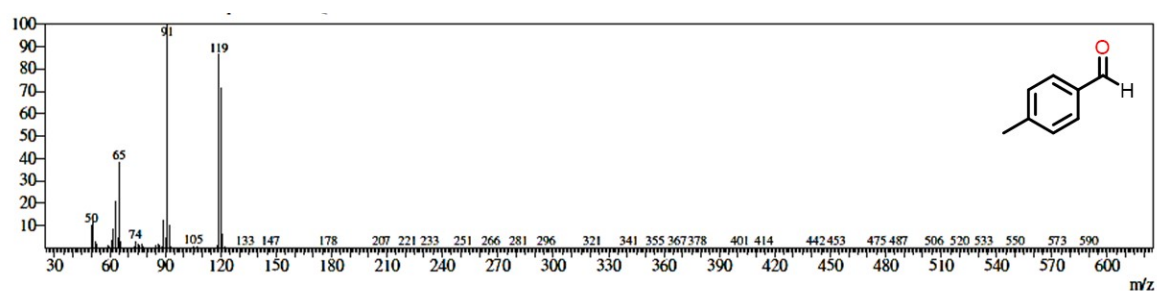


Fig. S7 GC-MS spectrum of 4-methylbenzaldehyde

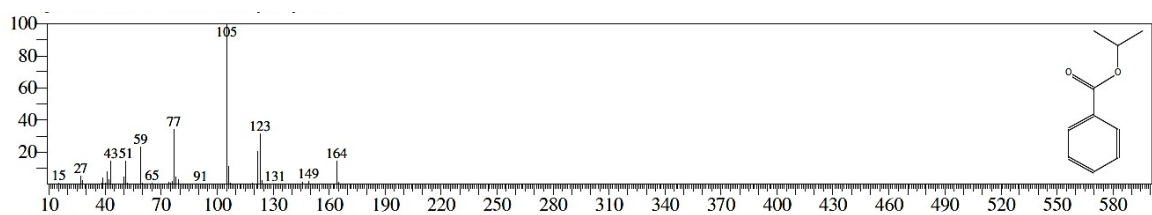


Fig. S8 GC-MS spectrum of isopropyl benzoate

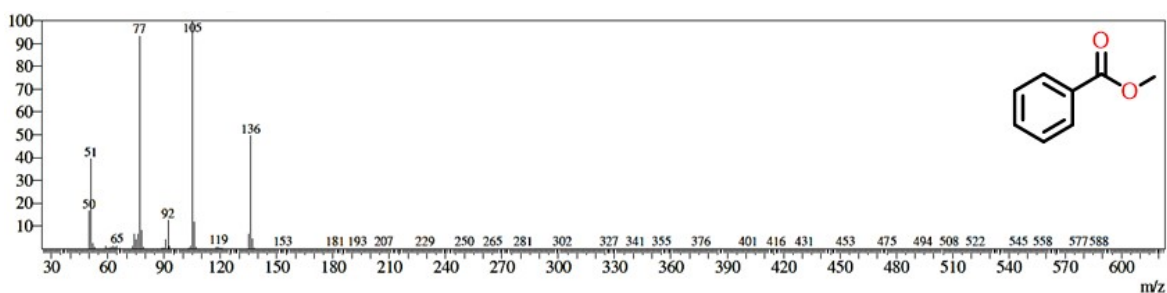
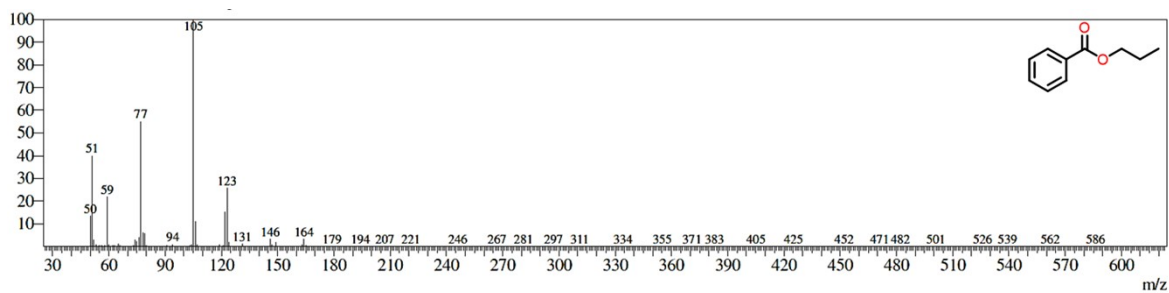
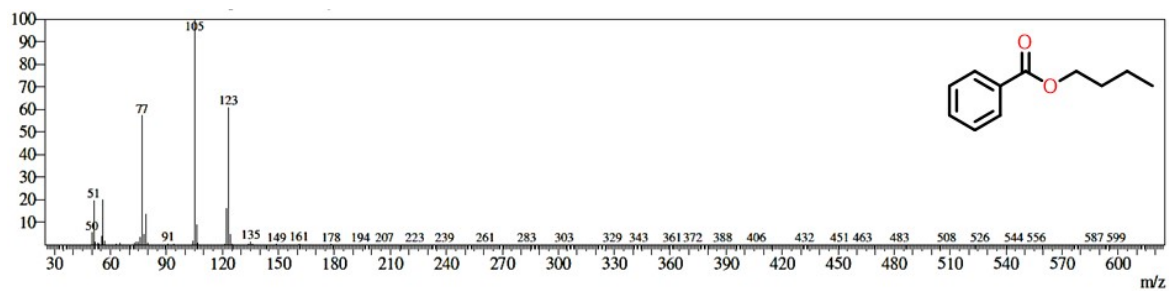


Fig. S9 GC-MS spectrum of methyl benzoate



**Fig. S10** GC-MS spectrum of propyl benzoate



**Fig. S11** GC-MS spectrum of butyl benzoate